

Chapter 4

Newtonian flow in blood vessels

4.1 Introduction

In this section the flow patterns in rigid straight, curved and branching tubes will be considered. First, fully developed flow in straight tubes will be dealt with and it will be shown that this uni-axial flow is characterized by two dimensionless parameters, the Reynolds number Re and the Womersley number α , that distinguish between flow in large and small vessels. Also derived quantities, like wall shear stress and vascular impedance, can be expressed as a function of these parameters.

For smaller tube diameters (micro-circulation), however, the fluid can not be taken to be homogeneous anymore and the dimensions of the red blood cells must be taken into account (see chapter 8). In the entrance regions of straight tubes, the flow is more complicated. Estimates of the length of these regions will be derived for steady and pulsatile flow.

The flow in curved tubes is not uni-axial but exhibits secondary flow patterns perpendicular to the axis of the tube. The strength of this secondary flow field depends on the curvature of the tube which is expressed in another dimensionless parameter: the Dean number. Finally it will be shown that the flow in branched tubes shows a strong resemblance to the flow in curved tubes.

4.2 Incompressible Newtonian flow in general

4.2.1 Incompressible viscous flow

For incompressible isothermal flow the density ρ is constant in space and time and the mass conservation or continuity equation is given by:

$$\nabla \cdot \mathbf{v} = 0 \quad (4.1)$$

In a viscous fluid, besides pressure forces also viscous forces contribute to the stress tensor and in general the total stress tensor can be written as (see chapter 2):

$$\boldsymbol{\sigma} = -p\mathbf{I} + \boldsymbol{\tau}(\dot{\mathbf{B}}). \quad (4.2)$$

In order to find solutions of the equations of motion the viscous stress tensor $\boldsymbol{\tau}$ has to be related to the kinematics of the flow by means of a constitutive equation depending on the rheological properties of the fluid. In this section only Newtonian fluids will be discussed briefly.

Newtonian flow

In Newtonian flow there is a linear relation between the viscous stress $\boldsymbol{\tau}$ and the rate of deformation tensor $\dot{\boldsymbol{\gamma}}$ according to:

$$\boldsymbol{\tau} = 2\eta\mathbf{D} = \eta\dot{\boldsymbol{\gamma}} \quad (4.3)$$

with η the dynamic viscosity and the rate of deformation tensor defined as:

$$\dot{\boldsymbol{\gamma}} = \nabla\mathbf{v} + (\nabla\mathbf{v})^c. \quad (4.4)$$

Substitution in the momentum equation yields the Navier-Stokes equations:

$$\begin{cases} \rho \frac{\partial \mathbf{v}}{\partial t} + \rho(\mathbf{v} \cdot \nabla)\mathbf{v} = \rho\mathbf{f} - \nabla p + \eta \nabla^2 \mathbf{v} \\ \nabla \cdot \mathbf{v} = 0 \end{cases} \quad (4.5)$$

After introduction of the non-dimensional variables: $\mathbf{x}^* = \mathbf{x}/L$, $\mathbf{v}^* = \mathbf{v}/V$, $t^* = t/\theta$, $p^* = p/\rho V^2$ and $\mathbf{f}^* = \mathbf{f}/g$, the dimensionless Navier-Stokes equations for incompressible Newtonian flow become (after dropping the superscript *):

$$\begin{cases} Sr \frac{\partial \mathbf{v}}{\partial t} + (\mathbf{v} \cdot \nabla)\mathbf{v} = \frac{1}{Fr^2}\mathbf{f} - \nabla p + \frac{1}{Re} \nabla^2 \mathbf{v} \\ \nabla \cdot \mathbf{v} = 0 \end{cases} \quad (4.6)$$

With the dimensionless parameters:

$$\begin{aligned} Sr &= \frac{L}{\theta V} && \text{Strouhal number} \\ Re &= \frac{\rho V L}{\eta} && \text{Reynolds number} \\ Fr &= \frac{V}{\sqrt{gL}} && \text{Froude number} \end{aligned} \quad (4.7)$$

4.2.2 Incompressible in-viscid flow

For incompressible isothermal flow the density ρ is constant in space and time and the mass conservation or continuity equation is given by:

$$\nabla \cdot \mathbf{v} = 0 \quad (4.8)$$

In an in-viscid fluid, the only surface force is due to the pressure, which acts normal to the surface. In that case the stress tensor can be written as:

$$\boldsymbol{\sigma} = -p\mathbf{I} \quad (4.9)$$

The momentum and continuity equations then lead to the Euler equations:

$$\begin{cases} \rho \frac{\partial \mathbf{v}}{\partial t} + \rho(\mathbf{v} \cdot \nabla)\mathbf{v} = \rho\mathbf{f} - \nabla p \\ \nabla \cdot \mathbf{v} = 0 \end{cases} \quad (4.10)$$

If the Euler equations are rewritten using the vector identity $(\mathbf{v} \cdot \nabla)\mathbf{v} = \frac{1}{2}\nabla(\mathbf{v} \cdot \mathbf{v}) + \boldsymbol{\omega} \times \mathbf{v}$ with the rotation $\boldsymbol{\omega} = \nabla \times \mathbf{v}$, an alternative formulation for the momentum equations then is given by:

$$\rho \frac{\partial \mathbf{v}}{\partial t} + \frac{1}{2}\rho\nabla(\mathbf{v} \cdot \mathbf{v}) + \boldsymbol{\omega} \times \mathbf{v} = \rho\mathbf{f} - \nabla p \quad (4.11)$$

It can readily derived that $\mathbf{v} \cdot (\boldsymbol{\omega} \times \mathbf{v}) = 0$ so taking the inner product of (4.11) with \mathbf{v} yields:

$$\mathbf{v} \cdot \left(\rho \frac{\partial \mathbf{v}}{\partial t} + \frac{1}{2}\rho\nabla(\mathbf{v} \cdot \mathbf{v}) - \rho\mathbf{f} + \nabla p \right) = 0 \quad (4.12)$$

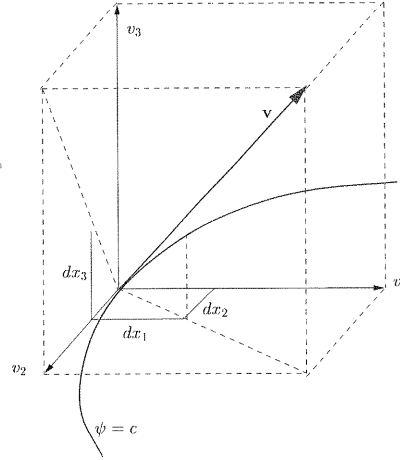


Figure 4.1: Definition of a streamline $\psi = c$.

Streamlines are defined as a family of lines that at time t is a solution of:

$$\frac{dx_1}{v_1(\mathbf{x}, t)} = \frac{dx_2}{v_2(\mathbf{x}, t)} = \frac{dx_3}{v_3(\mathbf{x}, t)} \quad (4.13)$$

As depicted in figure 4.1 the tangent of these lines is everywhere parallel to \mathbf{v} . If the flow is steady and only potential body forces $\mathbf{f} = -\nabla F$, like the gravity force \mathbf{g} , are involved, equation (4.12) yields

$$\mathbf{v} \cdot \nabla \left(\frac{1}{2} \rho (\mathbf{v} \cdot \mathbf{v}) + \rho F + p \right) \equiv \nabla H = 0 \quad (4.14)$$

As, by virtue of this, $\nabla H \perp \mathbf{v}$, along streamlines this results in the Bernoulli equation:

$$\frac{1}{2} \rho (\mathbf{v} \cdot \mathbf{v}) + p + \rho F = \text{const} \quad (4.15)$$

Irotational flow

For irrotational flow ($\boldsymbol{\omega} = \nabla \times \mathbf{v} = \mathbf{0}$) Bernoulli's equation holds for the complete flow domain. Moreover, since \mathbf{v} can be written as:

$$\mathbf{v} = \nabla \psi \text{ and thus due to incompressibility } \nabla^2 \psi = 0 \quad (4.16)$$

it follows that:

$$\rho \frac{\partial \psi}{\partial t} + \frac{1}{2} \rho (\mathbf{v} \cdot \mathbf{v}) + p + \rho F = \text{const} \quad (4.17)$$

Boundary conditions

Using the constitutive equation (4.9) the boundary conditions described in section 2.3.4 reduce to:

in normal direction:

$$\text{the Dirichlet condition: } (\mathbf{v} \cdot \mathbf{n}) = v_{n\Gamma}$$

$$\text{or Neumann condition: } (\boldsymbol{\sigma} \cdot \mathbf{n}) \cdot \mathbf{n} = p$$

in tangential directions:

$$\text{the Dirichlet conditions: } (\mathbf{v} \cdot \mathbf{t}_i) = v_{t_i\Gamma} \quad i = 1, 2$$

$$\text{or Neumann conditions: } (\boldsymbol{\sigma} \cdot \mathbf{n}) \cdot \mathbf{t}_i = 0$$

(4.18)

4.2.3 Incompressible boundary layer flow

Newtonian boundary layer flow

The viscous stress for incompressible flow

$$\boldsymbol{\tau} = \eta \dot{\boldsymbol{\gamma}} \quad (4.19)$$

is only large if velocity gradients are large especially if the viscosity is not too high. For flow along a smooth boundary parallel to the flow direction the viscous forces are only large in the boundary layer (see figure 4.2).

If the boundary layer thickness δ is small compared to a typical length scale of the flow an estimate of the order of magnitude of the terms and neglecting $\mathcal{O}(\delta/L)$ gives

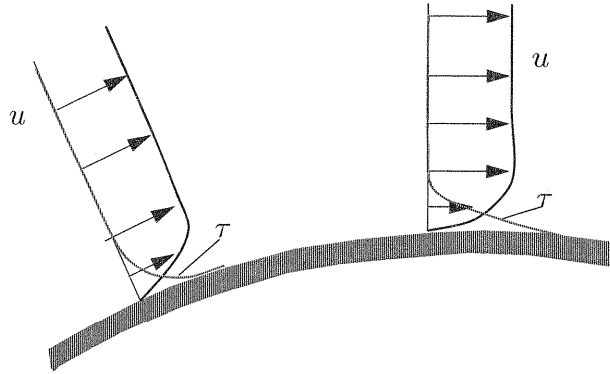


Figure 4.2: Velocity and stress distribution in a boundary layer.

the equations of motion:

$$\begin{cases} \frac{\partial v_1}{\partial x_1} + \frac{\partial v_2}{\partial x_2} = 0 \\ \rho \frac{\partial v_1}{\partial t} + \rho v_1 \frac{\partial v_1}{\partial x_1} + \rho v_2 \frac{\partial v_1}{\partial x_2} = -\frac{\partial p}{\partial x_1} + \eta \frac{\partial^2 v_1}{\partial x_2^2} \\ \frac{\partial p}{\partial x_2} = 0 \end{cases} \quad (4.20)$$

Outside the boundary layer the flow is assumed to be in-viscid and application of Bernoulli in combination with the second equation of (4.20) gives:

$$-\frac{\partial p}{\partial x_1} = \rho V \frac{\partial V}{\partial x_1} \quad (4.21)$$

Initial and boundary conditions

This set of equations requires initial conditions:

$$v_1(x_{10}, x_2, 0) = v_1^0(x_1, x_2) \quad (4.22)$$

and boundary conditions:

$$\begin{aligned} v_1(x_{10}, x_2, t) &= v_{10}(x_2, t) \\ v_1(x_1, 0, t) &= 0 \\ v_1(x_1, \delta, t) &= V(x_1, t) \end{aligned} \quad (4.23)$$

The boundary layer thickness δ can often be estimated by stating that at $x_2 = \delta$ the viscous forces $\mathcal{O}(\eta V / \rho \delta^2)$ are of the same magnitude as the stationary inertia forces $\mathcal{O}(V^2/L)$ or in-stationary inertia forces $\mathcal{O}(V/\theta)$.

4.3 Steady and pulsatile Newtonian flow in straight tubes

4.3.1 Fully developed flow

Governing equations

To analyze fully developed Newtonian flow in rigid tubes consider the Navier-Stokes equations in a cylindrical coordinate system:

$$\begin{cases} \frac{\partial v_r}{\partial t} + v_r \frac{\partial v_r}{\partial r} + v_z \frac{\partial v_r}{\partial z} = -\frac{1}{\rho} \frac{\partial p}{\partial r} + \nu \left(\frac{\partial}{\partial r} \left(\frac{1}{r} \frac{\partial}{\partial r} (r v_r) \right) + \frac{\partial^2 v_r}{\partial z^2} \right) \\ \frac{\partial v_z}{\partial t} + v_r \frac{\partial v_z}{\partial r} + v_z \frac{\partial v_z}{\partial z} = -\frac{1}{\rho} \frac{\partial p}{\partial z} + \nu \left(\frac{1}{r} \frac{\partial}{\partial r} \left(r \frac{\partial}{\partial r} (v_z) \right) + \frac{\partial^2 v_z}{\partial z^2} \right) \\ \frac{1}{r} \frac{\partial}{\partial r} (r v_r) + \frac{\partial v_z}{\partial z} = 0 \end{cases} \quad (4.24)$$

Since the velocity in circumferential direction equals zero ($v_\phi = 0$), the momentum equation and all derivatives in ϕ -direction are omitted. For fully developed flow the derivatives of the velocity in axial direction $\frac{\partial}{\partial z}$ and the velocity component in radial direction v_r are zero and equations (4.24) simplify to:

$$\frac{\partial v_z}{\partial t} = -\frac{1}{\rho} \frac{\partial p}{\partial z} + \frac{\nu}{r} \frac{\partial}{\partial r} \left(r \frac{\partial v_z}{\partial r} \right) \quad (4.25)$$

Now a dimensionless velocity can be defined as $v_z^* = v_z/V$, the coordinates can be made dimensionless using the radius of the tube, i.e. $r^* = r/a$ and $z^* = z/a$, the pressure can be scaled as $p^* = p/\rho V^2$ and the time can be scaled using $t^* = \omega t$. Dropping the asterix, the equation of motion reads:

$$\alpha^2 \frac{\partial v_z}{\partial t} = -Re \frac{\partial p}{\partial z} + \frac{1}{r} \frac{\partial}{\partial r} \left(r \frac{\partial v_z}{\partial r} \right) \quad (4.26)$$

with Re the Reynolds number given by

$$Re = \frac{aV}{\nu} \quad (4.27)$$

and α the Womersley number defined as:

$$\alpha = a \sqrt{\frac{\omega}{\nu}} \quad (4.28)$$

So two dimensionless parameters are involved : the Womersley number α defining the ratio of the instationary inertia forces and the viscous forces and the Reynolds number Re that is in this case nothing more then a scaling factor for the pressure gradient. The pressure could also be scaled according to $p^* = p/(a^2/\eta V)$ yielding one single parameter α .

In table 4.3.1 the Womersley numbers for several sites in the arterial system are given. These values show that in the aorta and in the largest arteries inertia dominated flow and in arterioles and capillaries friction dominated flow may be expected.

	a [mm]	α [-]
aorta	10	10
large arteries	4	4
small arteries	1	1
arterioles	0.1	0.1
capillaries	0.01	0.01

Table 4.1: Estimated Womersley number at several sites of the arterial system based on the first harmonic of the flow. A kinematic of $5 \cdot 10^{-3} [Pa \cdot s]$, a density of $10^3 [kg \cdot m^{-3}]$ and a frequency of $1 [Hz]$ are assumed.

In most part of the arteries an intermediate value of α is found and both inertia and viscous friction are important.

For the venous system a similar dependence of the Womersley number is found but it must be noted that inertia is less important due to the low amplitude of the first and higher harmonics with respect to the mean flow.

Velocity profiles

For flow in a rigid tube (see figure 4.3) with radius a the boundary condition $v(a, t) = 0$ is used to impose a no slip condition.

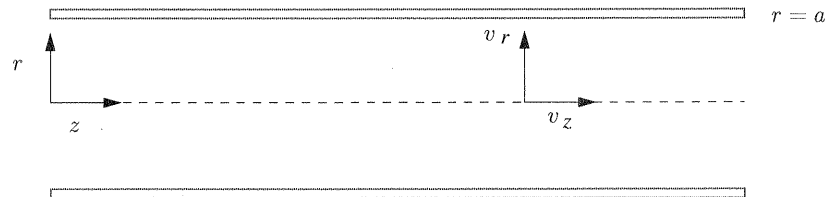


Figure 4.3: Rigid tube with radius a

We will assume a harmonic pressure gradient and will search for harmonic solutions:

$$\frac{\partial p}{\partial z} = \frac{\partial \hat{p}}{\partial z} e^{i\omega t} \quad (4.29)$$

and

$$v_z = \hat{v}_z(r) e^{i\omega t} \quad (4.30)$$

The solution of an arbitrary periodic function then can be constructed by superposition of its harmonics. This is allowed because the equation to solve (4.26) is linear in v_z .

Now two asymptotic cases can be defined. For small Womersley numbers there is an equilibrium of viscous forces and the driving pressure gradient. For large Womersley numbers, however, the viscous forces are small compared to the instationary inertia forces and there will be an equilibrium between the inertia forces and the driving pressure gradient. Both cases will be considered in more detail.

Small Womersley number flow. If $\alpha \ll 1$ equation (4.26) (again in dimension-full form) yields:

$$0 = -\frac{1}{\rho} \frac{\partial p}{\partial z} + \frac{\nu}{r} \frac{\partial}{\partial r} \left(r \frac{\partial v_z}{\partial r} \right) \quad (4.31)$$

Substitution of (4.29) and (4.30) yields:

$$\nu \frac{\partial^2 \hat{v}_z(r)}{\partial r^2} + \frac{\nu}{r} \frac{\partial \hat{v}_z(r)}{\partial r} = \frac{1}{\rho} \frac{\partial \hat{p}}{\partial z} \quad (4.32)$$

with solution:

$$v_z(r, t) = -\frac{1}{4\eta} \frac{\partial \hat{p}}{\partial z} (a^2 - r^2) e^{i\omega t} \quad (4.33)$$

So, for low values of the Womersley number a quasi-static Poiseuille profile is found. It oscillates 180° out of phase with the pressure gradient. The shape of the velocity profiles is depicted in the left graph of figure 4.4.

Large Womersley number flow. If the $\alpha \gg 1$ equation (4.26) yields:

$$\frac{\partial v_z}{\partial t} = -\frac{1}{\rho} \frac{\partial p}{\partial z} \quad (4.34)$$

Substitution of (4.29) and (4.30) yields:

$$i\omega \hat{v}_z(r) = -\frac{1}{\rho} \frac{\partial \hat{p}}{\partial z} \quad (4.35)$$

with solution:

$$v_z(r, t) = \frac{i}{\rho\omega} \frac{\partial \hat{p}}{\partial z} e^{i\omega t} \quad (4.36)$$

Now, for high values of the Womersley number, an oscillating plug flow is found which is 90° out of phase with the pressure gradient (right graph of figure 4.4). The flow is dominated by inertia.

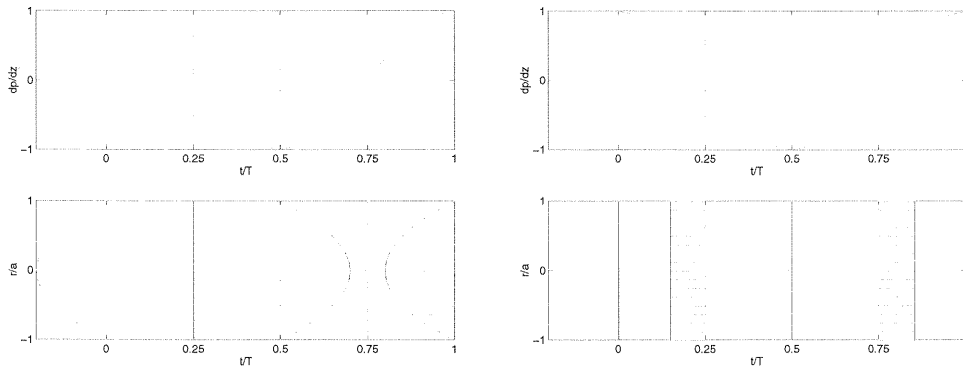


Figure 4.4: Pressure gradient (top) and corresponding velocity profiles (bottom) as a function of time for small (left) and large (right) Womersley numbers.

Arbitrary Womersley number flow. Substitution of (4.29) and (4.30) in equation (4.25) yields:

$$\nu \frac{\partial^2 \hat{v}_z(r)}{\partial r^2} + \frac{\nu}{r} \frac{\partial \hat{v}_z(r)}{\partial r} - i\omega \hat{v}_z(r) = \frac{1}{\rho} \frac{\partial \hat{p}}{\partial z} \quad (4.37)$$

Substitution of

$$s = i^{3/2} \alpha r / a \quad (4.38)$$

in the homogeneous part of this equation yields the equation of Bessel for $n = 0$:

$$\frac{\partial^2 \hat{v}_z}{\partial s^2} + \frac{1}{s} \frac{\partial \hat{v}_z}{\partial s} + \left(1 - \frac{n^2}{s^2}\right) \hat{v}_z = 0 \quad (4.39)$$

with solution given by the Bessel functions of the first kind:

$$J_n(s) = \sum_{k=0}^{\infty} \frac{(-1)^k}{k!(n+k)!} \left(\frac{s}{2}\right)^{2k+n} \quad (4.40)$$

so:

$$J_0(s) = \sum_{k=0}^{\infty} \frac{(-1)^k}{k!k!} \left(\frac{s}{2}\right)^{2k} = 1 - \left(\frac{s}{2}\right)^2 + \frac{1}{1^2 2^2} \left(\frac{s}{2}\right)^4 - \frac{1}{1^2 2^2 3^2} \left(\frac{s}{2}\right)^6 + \dots \quad (4.41)$$

(see Abramowitz and Stegun, 1964).

Together with the particular solution :

$$\hat{v}_z^p = \frac{i}{\rho \omega} \frac{\partial \hat{p}}{\partial z} \quad (4.42)$$

we have:

$$\hat{v}_z(s) = K J_0(s) + \hat{v}_z^p \quad (4.43)$$

Using the boundary condition $\hat{v}_z(a) = 0$ then yields:

$$K = -\frac{\hat{v}_z^p}{J_0(i^{3/2} \alpha)} \quad (4.44)$$

and finally:

$$\hat{v}_z(r) = \frac{i}{\rho \omega} \frac{\partial \hat{p}}{\partial z} \left[1 - \frac{J_0(i^{3/2} \alpha r / a)}{J_0(i^{3/2} \alpha)} \right] \quad (4.45)$$

These are the well known Womersley profiles (Womersley, 1957) displayed in figure 4.5. As can be seen from this figure, the Womersley profiles for intermediate Womersley numbers are characterized by a phase-shift between the flow in the boundary layer and the flow in the central core of the tube. Actually, in the boundary layer viscous forces dominate the inertia forces and the flow behaves like the flow for small Womersley numbers. For high enough Womersley numbers, in the central core, inertia forces are dominant and flattened profiles that are shifted in phase are found. The thickness of the instationary boundary layer is determined by the Womersley number. This will be discussed in more detail in section 4.3.2.

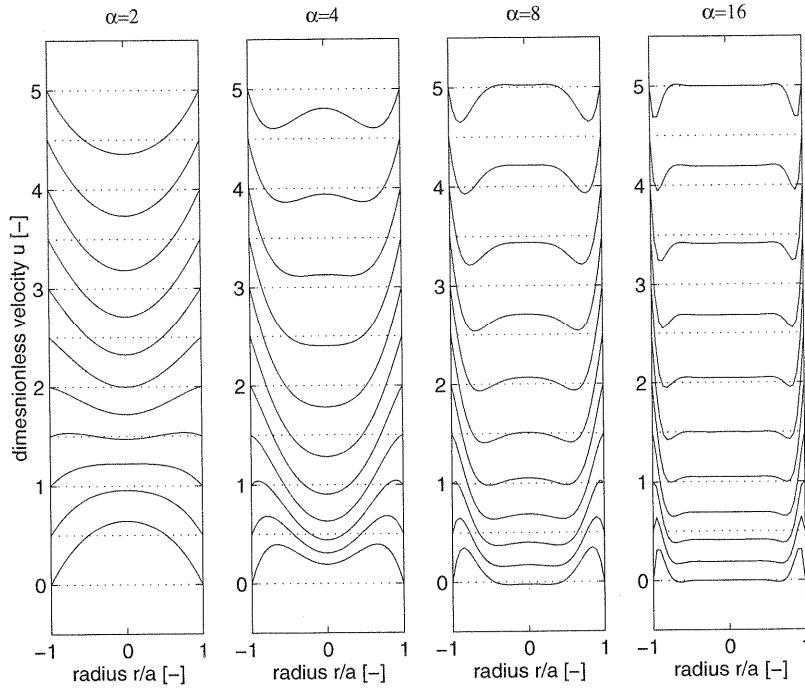


Figure 4.5: Womersley profiles for different Womersley numbers ($\alpha = 2, 4, 8, 16$)

Wall shear stress

Using the property of Bessel functions (see Abramowitz and Stegun, 1964)

$$\frac{\partial J_0(s)}{\partial s} = -J_1(s) \quad (4.46)$$

and the definition of the Womersley function

$$F_{10}(\alpha) = \frac{2J_1(i^{3/2}\alpha)}{i^{3/2}\alpha J_0(i^{3/2}\alpha)} \quad (4.47)$$

the wall shear stress defined as:

$$\tau_w = -\eta \frac{\partial v_z}{\partial r} \Big|_{r=a} \quad (4.48)$$

can be derived as:

$$\tau_w = -\frac{a}{2} F_{10}(\alpha) \frac{\partial p}{\partial z} = F_{10}(\alpha) \tau_w^p \quad (4.49)$$

with τ_w^p the wall shear stress for Poiseuille flow. In figure 4.6 the function $F_{10}(\alpha)$ and thus a dimensionless wall shear stress τ_w/τ_w^p is given as a function of α .

remark :

$$J_1(s) = \sum_{k=0}^{\infty} \frac{(-1)^k}{k!(1+k)!} \left(\frac{s}{2}\right)^{2k+1} = \left(\frac{s}{2}\right) - \frac{1}{1^2 2^2} \left(\frac{s}{2}\right)^3 + \frac{1}{1^2 2^2 3^2} \left(\frac{s}{2}\right)^5 + \dots \quad (4.50)$$

In many cases, for instance to investigate limiting values for small and large values of α , it is convenient to approximate the Womersley function with:

$$F_{10}(\alpha) \approx \frac{(1 + \beta)^{1/2}}{(1 + \beta)^{1/2} + 2\beta} \quad \text{with} \quad \beta = \frac{i\alpha^2}{16} \quad (4.51)$$

This approximation is plotted with dotted lines in figure 4.6. For small values of the Womersley number ($\alpha < 3$) the following approximation derived from (4.51) can be used:

$$F_{10}(\alpha) \approx \frac{1}{1 + 2\beta} = \frac{1}{1 + i\alpha^2/8} \quad (4.52)$$

whereas for large values ($\alpha > 15$) one may use:

$$F_{10}(\alpha) \approx \frac{1}{2}\beta^{-1/2} = \frac{(1 - i)\sqrt{2}}{\alpha} \quad (4.53)$$

These two approximations are plotted with dashed lines in figure 4.6. Note that the dimensionless wall shear stress for large values of α approximates zero and not ∞ that one could conclude from the steep gradients in the velocity profiles in figure 4.5.

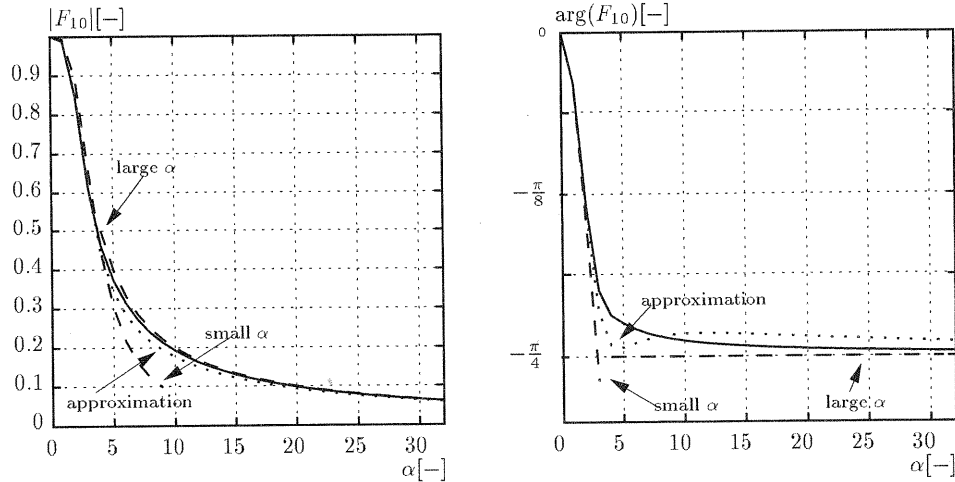


Figure 4.6: Modulus (left) and argument (right) of the function $F_{10}(\alpha)$ or τ_w/τ_w^p as a function of α . The approximations are indicated with dotted and dashed lines.

The mean flow q can be derived using the property (Abramowitz and Stegun, 1964):

$$s \frac{\partial J_n(s)}{\partial s} = -nJ_n(s) + sJ_{n-1}(s) \quad (4.54)$$

For $n = 1$ it follows that:

$$sJ_0(s)ds = d(sJ_1(s)) \quad (4.55)$$

and together with $J_1(0) = 0$ the flow becomes:

$$\begin{aligned}
 q &= \int_0^a \hat{v}_z 2\pi r dr = i \frac{\pi a^2}{\rho \omega} [1 - F_{10}(\alpha)] \frac{\partial p}{\partial z} \\
 &= [1 - F_{10}(\alpha)] \hat{q}_\infty \\
 &= \frac{8i}{\alpha^2} [1 - F_{10}(\alpha)] \hat{q}_p
 \end{aligned} \tag{4.56}$$

with

$$\hat{q}_\infty = \frac{i\pi a^2}{\rho \omega} \frac{\partial \hat{p}}{\partial z} \quad \text{and} \quad \hat{q}_p = \frac{\pi a^4}{8\eta} \frac{\partial \hat{p}}{\partial z} \tag{4.57}$$

Combining equation (4.49) with equation (4.56) by elimination of $\frac{\partial p}{\partial z}$ finally yields:

$$\tau_w = \frac{a}{2A} i\omega \rho \frac{F_{10}(\alpha)}{1 - F_{10}(\alpha)} q \tag{4.58}$$

With $A = \pi a^2$ the cross-sectional area of the tube. In the next chapter this expression for the wall shear stress will be used to approximate the shear forces that the fluid exerts on the wall of the vessel.

Vascular impedance

The longitudinal impedance defined as:

$$Z_L = -\frac{\partial p}{\partial z} / q \tag{4.59}$$

can be derived directly from equation (4.56) and reads:

$$Z_L = i\omega \frac{\rho}{\pi a^2} \frac{1}{1 - F_{10}(\alpha)} \tag{4.60}$$

For a Poiseuille profile the longitudinal impedance is defined by integration of (4.33) and is given by:

$$Z_p = \frac{8\eta}{\pi a^4} \tag{4.61}$$

From this it can be derived that the impedance of a rigid tube for oscillating flow related to the impedance for steady flow (Poiseuille resistance) is given by the following equation:

$$\frac{Z_L}{Z_p} = \frac{i\alpha^2}{8} \frac{1}{1 - F_{10}(\alpha)} \tag{4.62}$$

In figure 4.7 the relative impedance is plotted as a function of the Womersley number α . The relative longitudinal impedance is real for $\alpha \ll 1$ and becomes imaginary for $\alpha \rightarrow \infty$. This expresses the fact that for low frequencies (or small diameters)

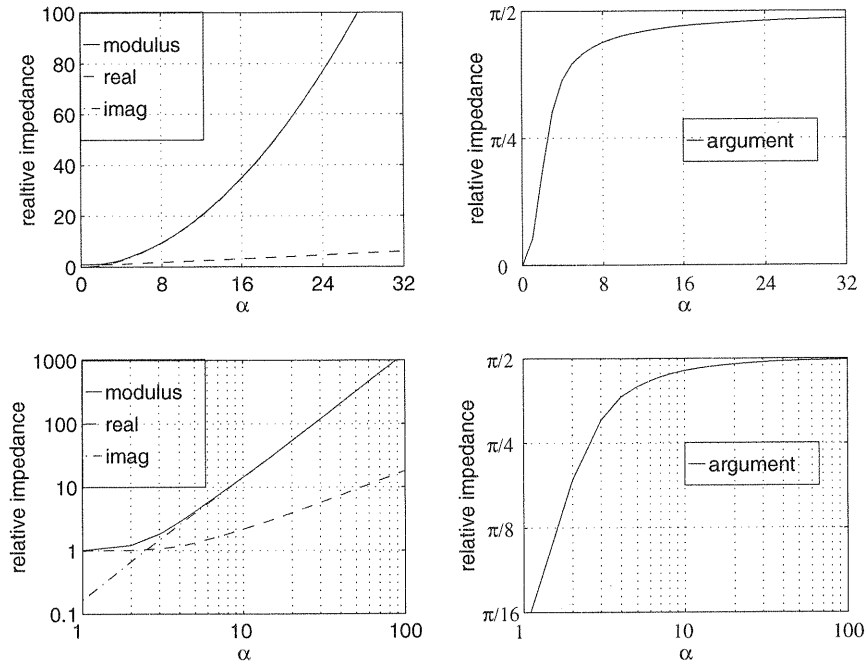


Figure 4.7: The relative impedance for oscillating flow in a tube (linear scale at the top and logarithmic scale at the bottom) as a function of α .

the viscous forces are dominant, whereas for high frequencies (or large diameters) inertia is dominant and the flow behaves as an inviscid flow.

For small values of α the relative impedance results in (see 4.52):

$$\frac{Z_L(\alpha < 3)}{Z_p} \approx 1 + \frac{i\alpha^2}{8} \quad (4.63)$$

Viscous forces then dominate and the pressure gradient is in phase with the flow and does not (strongly) depend on α . For large values of α (4.53) gives:

$$\frac{Z_L(\alpha > 15)}{Z_p} \approx \frac{i\alpha^2}{8} \quad (4.64)$$

indicating that the pressure gradient is out of phase with the flow and increases quadratically with α .

4.3.2 Entrance flow

In general the flow in blood vessels is not fully developed. Due to transitions and bifurcations the velocity profile has to develop from a certain profile at the entrance of the tube (see figure 4.8).

In order to obtain an idea of the length needed for the flow to develop, the flow with a characteristic velocity V along a smooth boundary with characteristic length L is

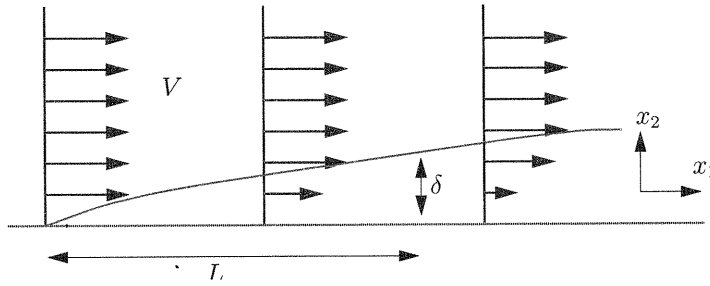


Figure 4.8: Development of a boundary layer

considered. Viscous forces only play an important role in the small boundary layer with thickness δ . Outside the boundary layer the flow is assumed to be inviscid so that Bernoulli's law can be applied. From this configuration simplified Navier-Stokes equations can be derived by assuming that $\delta \ll L$ (see 4.20) and the order of magnitude of its terms can be estimated:

$$\left\{ \begin{array}{l} \frac{\partial v_1}{\partial x_1} + \frac{\partial v_2}{\partial x_2} = 0 \\ O\left(\frac{V}{L}\right) \quad O\left(\frac{v}{\delta}\right) \\ \rho \frac{\partial v_1}{\partial t} + \rho v_1 \frac{\partial v_1}{\partial x_1} + \rho v_2 \frac{\partial v_1}{\partial x_2} = -\frac{\partial p}{\partial x_1} + \eta \frac{\partial^2 v_1}{\partial x_1^2} + \eta \frac{\partial^2 v_1}{\partial x_2^2} \\ O(\omega V) \quad O\left(\frac{V^2}{L}\right) \quad O\left(\frac{V^2}{L}\right) \quad O\left(\frac{1}{\rho} \frac{\partial p}{\partial x}\right) \quad O\left(\frac{\nu V}{L^2}\right) \quad O\left(\frac{\nu V}{\delta^2}\right) \end{array} \right. \quad (4.65)$$

This shows clearly that the diffusive forces are determined by second order derivatives of the velocity normal to the boundary. Moreover it can be seen that the stationary inertia forces are of the same order of magnitude as the viscous forces (which is the case at the boundary layer $x_2 = \delta$) as long as:

$$O\left(\frac{\nu V}{\delta^2}\right) = O\left(\frac{V^2}{L}\right) \quad (4.66)$$

Steady flow

If the entrance length of the flow in a tube is defined as the length needed for the boundary layer to contain the complete cross section, i.e. $\delta = a$, then the ratio of the entrance length and the radius of the tube follows from the equation above as:

$$\frac{L_e}{a} = O\left(\frac{aV}{\nu}\right) \quad (4.67)$$

Or with the definition of the Reynolds number $Re = 2aV/\nu$ the dimensionless entrance length $L_e/2a$ is found to be proportional to the Reynolds number:

$$\frac{L_e}{2a} = O(Re) \quad (4.68)$$

In Schlichting (1960) one can find that for laminar flow, for $L_e : v(L_e, 0) = 0.99 \cdot 2V$:

$$\frac{L_e}{2a} = 0.056 Re \quad (4.69)$$

For steady flow in the carotid artery, for instance, $Re = 300$, and thus $L_e \approx 40a$. This means that the flow will never become fully developed since the length of the carotid artery is much less than 40 times its radius. In arterioles and smaller vessels, however, $Re < 10$ and hereby $L_e < a$, so fully developed flow will be found in many cases.

Oscillating flow

For oscillating flow the inlet length is smaller as compared to the inlet length for steady flow. This can be seen from the following. The unsteady inertia forces are of the same magnitude as the viscous forces when:

$$O(V\omega) = O\left(\frac{\nu V}{\delta^2}\right) \quad (4.70)$$

and thus:

$$\delta = O\left(\sqrt{\frac{\nu}{\omega}}\right) \quad (4.71)$$

This means that for fully developed oscillating flow a boundary layer exists with a relative thickness of:

$$\frac{\delta}{a} = O(\alpha^{-1}) \quad (4.72)$$

If, for oscillating flow, the inlet length is defined as the length for which the viscous forces still are of the same magnitude as the stationary inertia forces, i.e.:

$$O\left(\frac{\nu V}{\delta^2}\right) = O\left(\frac{V^2}{L_e}\right) \quad (4.73)$$

then together with (4.72) the inlet length is of the order

$$L_e = O\left(\frac{V\delta^2}{\nu}\right) = O\left(\frac{a}{\alpha^2} Re\right) \quad (4.74)$$

Note that this holds only for $\alpha > 1$. For $\alpha < 1$ the boundary layer thickness is restricted to the radius of the tube and we obtain an inlet length of the same magnitude as for steady flow.

4.4 Steady and pulsating flow in curved and branched tubes

4.4.1 Steady flow in a curved tube

Steady entrance flow in a curved tube

The flow in a curved tube is determined by an equilibrium of convective forces, pressure forces and viscous forces. Consider, the entrance flow in a curved tube